The Journal of Experimental Biology 207, 2455-2464
Published by The Company of Biologists 2004
doi:10.1242/jeb.01039

Cardiac-like behavior of an insect flight muscle

Michael S. Tu* and Thomas L. Daniel
Department of Biology, University of Washington, Seattle, WA 98195-1800, USA
*Author for correspondence (e-mail: mstu@u.washington.edu)

Accepted 20 April 2004

Summary

The synchronous wing depressor muscles of the hawkmoth *Manduca sexta* undergo large amplitude motions at lengths that lie entirely on the ascending region of their twitch length–tension curve. Moreover, these muscles bear a striking functional resemblance to mammalian cardiac muscle in both the shape of their length–tension curve and in their working length range. Although operation on the ascending region of the twitch length–tension curve sacrifices maximal force, it does permit the generation of larger forces at greater strains. In the case of cardiac muscle, this mechanical behavior is critical for accommodating the increasing stresses associated with greater ventricular filling. Similar characteristics in moth flight muscle suggest an analogous regulatory mechanism for skeletal muscles performing repetitive oscillatory work; the strong length dependence of force over their working length range should give the wing depressors the capacity to generate larger forces as wing stroke amplitude increases. These results support the notion that the length–tension relationship of muscle can be tuned to function in locomotor muscles.

Key words: flight, strain, *Manduca sexta*, length–tension, muscle.

Introduction

Forces generated by both skeletal and cardiac muscle depend strongly upon muscle length. The *in vivo* range of lengths is therefore a critical determinant of muscle performance. On the classic sarcomere length–tension curve (Gordon et al., 1966), force peaks at lengths corresponding to nearly complete overlap of the thick and thin filaments. In locomotor muscles, length changes could straddle the peak of force generation, lie along the ascending portion or lie along the descending portion of the length–tension curve. Identifying the operating length ranges of muscles and understanding their functional consequences are both central to studies of muscle physiology in locomotion.

For flying animals, *in vivo* length changes of muscles have been measured for birds (Biewener et al., 1998; Dial and Biewener, 1993; Williamson et al., 2001) and for asynchronous flight muscles in insects (bumblebees – Gilmour and Ellington, 1993; Josephson and Ellington, 1997; *Drosophila* – Chan and Dickinson, 1996). These studies, however, do not locate the *in vivo* operating length range with respect to each muscle's length–tension curve. More data are available for estimates of *in vivo* sarcomere length ranges during terrestrial locomotion and swimming (reviewed by Burkholder and Lieber, 2001). However, these measurements are all referenced to the skeletal muscle length–tension curve measured for frog leg muscles by Gordon et al. (1966). Two issues potentially confound previous analyses. First, the shape, and particularly the steepness, of the length–tension curve depends strongly on the level of muscle activation (Rack and Westbury, 1969). Because few muscles are maximally activated during locomotion, estimates of the *in vivo* operating range of a muscle referenced to the length–tension curve for tetanically activated muscles may not accurately reflect *in vivo* performance. Second, variation in filament geometry cannot account for all of the known variation in the length–tension relationship, in particular the well-known differences between curves for cardiac and skeletal muscles (Allen and Kentish, 1985; Layland et al., 1995).

Despite the importance of the operating length range, there are surprisingly few studies in which the *in vivo* length changes of a locomotor muscle have been mapped onto its own length–tension relationship measured at levels of activation similar to those that occur during locomotion. Such measurements are technically challenging, and many muscles, such as those in arms, fins and legs, generate and control motions that are highly variable and complex. The resulting uncertainty in operating length complicates analyses of structural adaptations and performance. On the other hand, muscles that are restricted to repetitive length changes at relatively constant frequency and amplitude may represent simpler cases that may more readily yield insights into muscle design.

Cardiac muscle is one case where the functional consequences of operating length are well known. Three emergent properties are critical for cardiac muscle performance: (1) cardiac muscles operate at strains as high as 10% (Layland et al., 1995); (2) such strains occur at sarcomere lengths that lie entirely on the ascending portion of the cardiac length–tension relationship (Layland et al., 1995) and (3)

compared with skeletal muscle, cardiac muscle shows an exceptionally steep length–tension relationship that cannot be accounted for solely by the changes in myofilament overlap (Allen and Kentish, 1985; Layland et al., 1995). In addition to geometric components, regulatory factors such as the particular troponin isoform can affect the steepness of the force–length relationship (Gordon et al., 2000). Regardless of the underlying mechanisms, however, the steep length–tension relationship clearly plays a crucial role in cardiac muscle performance. Regulation of cardiac output by changes in end-diastolic volume, as described by the Frank–Starling principle, requires greater muscle forces to accommodate greater ventricular filling. Operation at lengths that lie on the ascending portion of a steeply rising length–tension curve gives cardiac muscle the capacity to generate these larger stresses as the ventricle walls stretch (Allen and Kentish, 1985; Layland et al., 1995). The possibility that skeletal muscles might also exploit these design principles has not been explored. Because the muscles that power insect flight also undergo relatively constant, cyclic length oscillations, we were intrigued by the possibility that insect flight muscle and mammalian cardiac muscle may share fundamental mechanical characteristics.

Insects have evolved two distinct types of flight muscle. One type, asynchronous muscle, powers flight in many small insects (e.g. Diptera, Hymenoptera). Here, decoupling between the timing of neuronal activation and muscle contraction permits high-frequency contractions without the need for elaborate internal membrane systems for calcium cycling (Josephson et al., 2000). Asynchronous flight muscle is a unique and critical adaptation that permits high power output at high contraction frequencies, within the stringent weight and volume constraints imposed on small flying insects. Many insects, however, power flight with synchronous muscle. In these muscles, as in the flight muscles of bats and birds, muscle contraction is directly coupled to motor axon activation. Insects with synchronous flight muscle therefore offer an opportunity to draw parallels between insect and vertebrate fliers as we seek to understand general design principles for animal flight. Central to this effort are detailed analyses of the patterns of force production and strain.

Here, for a synchronous insect flight muscle, the mesothoracic dorsolongitudinal muscles (dl_1 muscles; Nüesch, 1953; Eaton, 1988) of the hawkmoth *Manduca sexta*, we report both *in vivo* muscle length changes and the length dependence of isometric twitch forces measured using a physiologically appropriate level of stimulation. We use these data to determine the *in vivo* operating length range of the dl_1 muscles relative to their active twitch length–tension relationship. In a subsequent paper (M.S.T. and T.L.D., in preparation), we examine the effects of mean operating length, strain amplitude and phase of activation on the mechanical power output of the dl_1 muscles.

The dl_1 muscles of *Manduca* provide an ideal system for addressing questions of muscle design. These synchronous muscles power the downstroke of the wings. Like cardiac muscles, the dl_1 muscles drive highly repetitive motions. Alterations in wing stroke kinematics appear to be accomplished by a separate, anatomically distinct set of steering muscles (Kammer, 1985). The ability to reliably define a reference length is critical for any analysis of length effects on muscle function. Fortunately, while at rest, *Manduca* assume a stereotyped posture with their wings folded back over their body. This behavior allowed us to unambiguously identify a consistent anatomical rest length, L_r, of the dl_1 muscles. In this study, we measure length changes of the dl_1 muscles in tethered flight and map these length changes onto their isometric twitch length–tension curve. Because the dl_1 muscles are typically activated once in each wing stroke (Kammer, 1971; Rheuben and Kammer, 1987; Wendler et al., 1993), we measure the isometric twitch length–tension curve rather than a length–tension curve based on tetanic force.

Materials and methods

Animals and muscles

Adult *Manduca sexta* L. were obtained from a colony maintained in the Department of Biology at the University of Washington. Larvae were raised on artificial diet at 26°C. Both larvae and adults were maintained under a 17 h:7 h L:D photoperiod. We shifted the photoperiod of the moths so that the onset of their dark period occurred in mid-morning. Adults were used within 1–3 days of eclosion.

The dl_1 muscles span the length of the mesothorax and attach to the 1st and 2nd phragmata (Fig. 1). The phragmata are deep invaginations of the dorsal exoskeleton that form broad areas for muscle attachment. Each of the bilaterally paired dl_1 muscles consists of five sub-units designated, from ventral to dorsal, dl_{1a} to dl_{1e} (Nüesch, 1953; Eaton, 1988).

Experimental approach

Due to anatomical constraints and the conflicting characteristics of the instrumentation required to measure *in vivo* length changes and isometric force, we could not perform all measurements on the same individual moths. We therefore used a two-pronged approach. First, during tethered flight, we measured the amplitude of muscle length changes and the mean operational length, both referenced to the anatomical rest length (Fig. 1). Second, in a group of intact moths, we measured the active component of the isometric twitch force to generate the isometric twitch length–tension curve for the dl_1 muscles (Fig. 1). As with the measurements of length changes during tethered flight, these length–tension measurements were also referenced to the anatomical rest length. Using the anatomical rest length as a reference for both sets of measurements enabled us to map *in vivo* length changes during flight onto the isometric twitch length–tension curve.

Preservation of this reference length in our active twitch length–tension measurements required that we leave the exoskeleton intact. Because we measured only the active component of muscle twitch force, our measurements were not contaminated by the steady-state stress in the exoskeleton due to imposed changes in muscle length. To assess the extent to

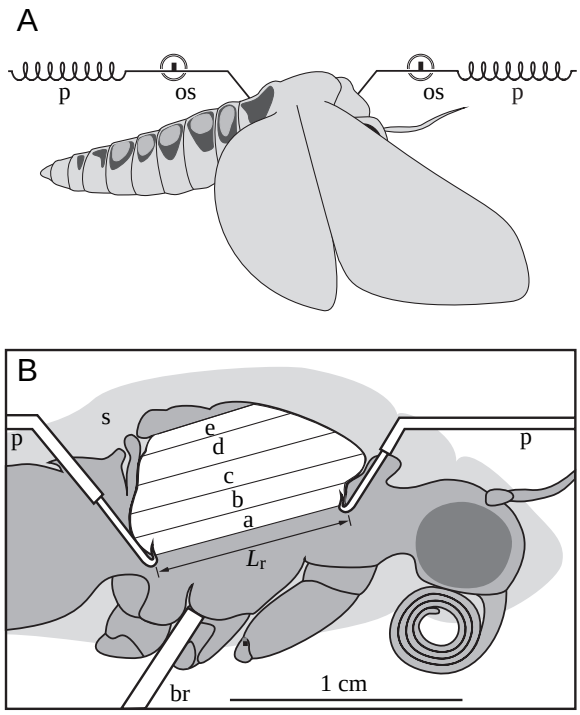

Fig. 1. Preparation for measurement of muscle length changes during tethered flight and length–tension measurements in the intact thorax. (A) Lateral view of *Manduca* showing placement of length transducer probes (p) and optical sensors (os) used to measure length changes of the dl_1 muscles during tethered flight. (B) The five subunits of each dl_1 muscle (a–e) attach to two invaginations of the exoskeleton, the 1st phragma anteriorly and the 2nd phragma posteriorly. Acting indirectly through a complex wing articulation, contraction of the dl_1 muscles depresses the wings. The probes were inserted through incisions in membranous areas of the abdomen and neck and hooked onto the 1st and 2nd phragmata. The moth was held on a brass rod (br) glued between the bases of the mesothoracic legs. We define the anatomical rest length, L_r, as the length of dl_{1a} along its ventral surface in the intact thorax of a quiescent moth. In practice, we measured L_r as the distance separating the hooks of the displacement transducer probes with the moth at rest. For isometric twitch length–tension measurements in the intact thorax, the probe hooks were bilaterally paired rather than single, but the method of insertion and placement was the same. The anterior probe was rigidly fixed in place, and the posterior probe was connected to an isometric force transducer. s, silhouette of body scales.

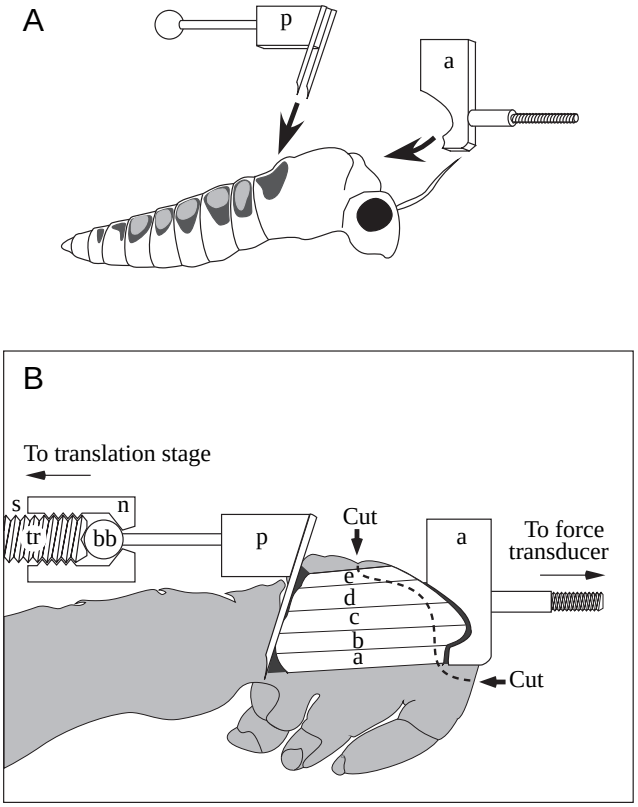

Fig. 2. Preparation used to measure isometric twitch forces from mechanically isolated dl_1 muscles. (A) Placement of the anterior (a) and posterior (p) muscle grips for twitch force measurements on mechanically isolated muscles. (B) After decapitating the moth, the 1st phragma was exposed and the anterior grip placed over the anterior insertion of the dl_1 muscles. The paired needles of the posterior grip were driven through the dorsal cuticle and down along the posterior face of the 2nd phragma. Both grips were secured to the exoskeleton with cyanoacrylate adhesive. After gluing acetate strips (not shown) across the gap between the two grips to fix their relative positions, cuticle strips were excised (arrows, broken line) to mechanically isolate the anterior grip and muscle insertions from the rest of the thorax. The anterior grip was then secured to the force transducer *via* the threaded rod projecting from the grip. The ball bearing (bb) mounted on the posterior grip fit into a depression in the end of a threaded rod (tr) mounted on a translation stage. When secured by a slotted retaining nut (n), the ball bearing and threaded rod formed a ball joint. The acetate strips spanning the two grips were then cut, and any misalignment of the cut ends was corrected using the ball joint and translation stage.

which the intact exoskeleton may have altered the shape of the measured twitch length–tension curve, we performed a second set of twitch length–tension measurements on mechanically isolated muscles (Fig. 2). The measurements on mechanically isolated muscles also permitted force measurements over a larger range of length than was possible in the intact thorax.

Muscle strain and activation phase during tethered flight

Moth preparation

We prepared moths under normal room light near the end of the light phase of their photoperiod. Moths were immobilized by 1–2 min of exposure to CO_2. We rubbed off the scales of the meso- and metathoracic coxae and glued a tapered brass rod between the coxae with cyanoacrylate adhesive. The rod was then clamped with the longitudinal body axis of the moth oriented horizontally. Tethered flight data were recorded under low light conditions during the first 1–3 h of the moth's normal period of darkness, 2–3 h following CO_2 exposure.

Length transducers

We measured length changes of the dl_1 muscles by tracking the motions of the 1st and 2nd phragmata simultaneously. We

used two displacement transducers, each consisting of a spring with a probe attached to its free end (Fig. 1). The probes were constructed from 0.78 mm-diameter stainless steel hypodermic tubing. Each ended in a small, upturned hook. We used optical sensors (Spot 2D; UDT Sensors Inc., Hawthorne, CA, USA) paired with red light-emitting diodes (LEDs) to track the motion of a small metal flag soldered to the base of each probe. The fixed end of each probe, together with its associated sensor, was mounted on a linear translation stage. To calibrate each transducer, the hook was clamped to a fixed reference, and the voltage output of the optical sensor amplifier circuit was recorded as the translation stage was moved in known increments. The micrometer of the translation stage allowed us to calibrate each displacement transducer to a precision of 10 μm.

The anterior probe was hooked onto the ventral margin of the 1st phragma through a short, transverse incision in the membranous region just anterior to the metathoracic prescutum. We inserted the probe of the posterior displacement transducer through a narrow slit cut in the soft cuticle along the dorsal midline of the first two abdominal segments. This probe deflected the heart to one side, passed through a large abdominal air sac, and hooked onto the ventral margin of the 2nd phragma. Coupled motion of the wings and probes indicated successful attachment of the probes.

The anterior and posterior displacement transducers had unloaded resonant frequencies of 50 and 40 Hz, respectively, well above the typical wing-beat frequency of approximately 25 Hz. Both transducers had a compliance of 0.01 m N^{-1}. Based on subsequent measurements of twitch forces, tension imposed on the dl_1 muscles by the displacement transducers was maximally 6% of the peak isometric twitch force when the muscle was stretched by 10% of its resting length.

To maintain stable contact with the phragmata, we positioned each transducer so that its spring was under light tension. This tension was not high enough, however, to alter the rest position of the wings. To further verify that the tension in the displacement transducers did not change the rest length of the muscles, we performed dissections on several moths to expose the ventral surface of the dl_1 muscles, with the displacement transducers attached. Stretching the springs of the displacement transducers to lengths beyond those observed in flight did not produce visible movements of the phragmata, indicating that the tension in the transducers did not bias our measurements of muscle length.

EMG recordings

We performed differential EMGs from the left dl_{1c} because it is the largest sub-unit that is directly accessible through the scutum. We used pairs of electrodes fashioned from short lengths of 25.4 μm formvar-insulated Nichrome wire (38.1 μm outside diameter; A-M Systems, Carlsborg, WA, USA), with the insulation cut flush with the end of the wire. After removing the scales covering the anterior insertion of dl_{1c}, we implanted both electrodes through holes in the cuticle made by a minuten pin. Extracellular potentials were amplified using a differential AC amplifier (Model 1700; A-M Systems) and band pass filtered (0.3–20 kHz).

Data acquisition and analysis

We recorded extracellular potentials and muscle length changes using a 16-bit analog-to-digital converter interfaced with a computer. Each data channel was digitized at a rate of 4 kHz. We simultaneously recorded all trials on video tape at 30 frames s^{-1} using a digital video camera. The video camera was oriented perpendicular to the sagittal plane of the moth. A mirror placed at a 45° angle in front of the moth provided a view of the wing stroke in the transverse plane. An LED placed in the video field was illuminated during data acquisition and allowed us to synchronize the computer and video recordings.

We define the anatomical rest length, L_r, as the length of dl_{1a} along its ventral surface in the intact thorax of a quiescent moth. We measured L_r in tethered flight preparations as the distance separating the hooks of the displacement transducer probes (Fig. 1). At the end of a recording session, we fixed the distance between the hooks by gluing two strips of acetate transparency film across the space separating the two probes. The acetate strips held the probes in position while we disengaged the probes from the phragmata and removed the moth from the apparatus. We then measured L_r to the nearest 0.05 mm.

For each sample period in the muscle length recordings, we calculated the instantaneous length of the muscle as the sum of L_r and the combined displacements of the 1st and 2nd phragmata away from their rest positions. Each strain cycle was defined as the time separating successive minima in the strain record. Wing-beat frequency was calculated for each cycle and averaged across the total number of complete cycles in each flight sequence. We defined the operational muscle length, L_{op}, for each cycle as the midpoint between the maximum (L_{up}) and minimum (L_{dn}) length of the muscle in that cycle: $L_{op}=(L_{up}+L_{dn})/2$. We calculated strain amplitude as the total fractional change in muscle length in each cycle, normalized to the operational length: strain$=(L_{up}-L_{dn})/L_{op}$. We then averaged values of strain amplitude and L_{op} across all wing-strokes of each flight bout. We calculated the phase of activation of the dl_1 muscles as the time from the start of muscle lengthening to the peak of the spike in the subsequent extracellular spike, divided by the cycle period.

Isometric twitch and twitch length–tension measurements

Force transducer

The force transducer consisted of a cantilevered 6.25×1.5 mm brass beam with a free length of 35.25 mm. We used an optical sensor (Spot 2D; UDT Sensors Inc.) to track the position of a short length of stainless steel hypodermic tubing soldered to the end of the beam. The force beam had a compliance of 3.6×10^{-4} m N^{-1} and an unloaded resonant frequency of 640 Hz. The force transducer was mounted on a 3-axis micromanipulator, which in turn was mounted on a linear translation stage. Using the calibrated micrometer on the translation stage, we could adjust the force transducer position with a precision of 0.01 mm.

Intact thorax preparation

To measure the isometric twitch length–tension curve in intact moths, we prepared moths as described for tethered flight experiments. As in the tethered flight preparation, the phragmata were secured to hooks inserted through dorsal incisions in the prothorax and abdomen. The hooks differed from those used for strain measurements in that they were bilaterally paired to avoid slipping or tearing the cuticle as the muscles twitched. Instead of using compliant displacement transducers, the probe hooked onto the anterior phragma was rigidly fixed in place, and the posterior probe was connected directly to the force transducer.

Any disruption of the thoracic exoskeleton invariably alters the resting length of the muscles. Consequently, with the exception of the incisions in soft tissue of the prothorax and abdomen required to insert the displacement transducer probes, we left the thoracic exoskeleton completely intact. We also monitored wing posture to detect any changes in the relative positions of the phragmata that occurred when we attached the hooks. We removed any length offset introduced during hook placement by adjusting the hook position until the wings assumed their normal resting posture.

Isolated muscle preparation

The dl_1 muscles receive their primary respiratory air supply from large tracheal trunks originating at the mesothoracic spiracles. On each side of the moth, these tracheal trunks run anteriorly between the dl_1 muscles and the dorsoventral muscles, supplying both muscle groups. This arrangement of tracheae made it impossible to remove the dl_1 muscles from the thorax without compromising their oxygen supply. In addition, respiratory pumping by the abdomen appears critical for prolonged viability of the dl_1 muscles; muscle performance deteriorated rapidly if we removed the abdomen in order to expose the posterior muscle attachments on the 2nd phragma. We therefore developed a semi-intact preparation that minimized the dissection necessary to mechanically isolate the dl_1 muscles between two specially constructed grips (Fig. 2).

The anterior grip consisted of a small aluminum block shaped to match the contours of the anterior mesoscutum and the 1st phragma (Fig. 2). Each moth was immobilized by brief (1–2 min) exposure to CO_2, decapitated, and the scales rubbed off from the dorsal surfaces of the thorax. Once the thoracic exoskeleton is cut to mechanically isolate the dl_1 muscles, wing position no longer serves as a reliable indicator of rest length. We therefore removed the wings to facilitate the muscle preparation. The 1st phragma was exposed by severing the pronotum near its articulation to the mesothoracic prescutum and by clearing away the prothoracic dorsolongitudinal muscles. After scraping away the waxy epicuticle, we used cyanoacrylate adhesive to attach the grip to the cuticle overlying the anterior origins of the dl_1 muscles. Any gaps between the grip and the exoskeleton were filled with a composite formed from cyanoacrylate and sodium bicarbonate powder.

The posterior grip consisted of a pair of 0.68 mm-diameter stainless steel hypodermic needles soldered to a small brass block (Fig. 2). The needles were parallel to each other and were separated by a distance slightly less than the lateral width of the 2nd phragma. A drop of cyanoacrylate adhesive was placed in the deep groove overlying the phragma. We then pushed the needles down into the groove so that they punctured the metathoracic scutellum and passed down along the posterior face of the phragma. Cyanoacrylate flowing between the needles and the cuticle solidly bonded the phragma and scutellum to the needles and brass block. We discarded trials if dissection following the measurements showed that the needles had pierced the phragma, or if the needles and phragma were not solidly bonded.

To preserve the orientation of the dl_1 muscles as the thorax was transferred to the experimental apparatus, we glued two strips of acetate transparency film, one strip on each side, across the gap separating the two grips. The acetate strips restricted length changes and prevented bending and torsion of the muscles. We then excised a thin strip of cuticle from around the anterior grip. After cutting away this strip of cuticle, the dl_1 muscles and the acetate strips glued to the grips were the only remaining mechanical links between the anterior and posterior attachments of the muscles.

The anterior grip was attached to the force beam *via* a short, threaded steel rod projecting from the front of the grip. The threaded end of the rod was inserted through a hole near the end of the force beam and secured with a nut. The posterior grip was attached to a linear translation stage. A short length of stainless steel tubing projected from the back of the grip and terminated in a ball bearing. The ball bearing fit into a depression at the end of a threaded rod rigidly fixed to the translation stage. The threaded rod and the ball bearing formed a ball joint when secured with a slotted retaining nut.

Once the two grips were secured, we cut the acetate strips connecting the two grips, leaving the dl_1 muscles as the only direct mechanical linkage between the fixed posterior section of the thorax, and the anterior muscle attachments connected to the force beam. Cutting the acetate strips also relieved any stresses induced in the thorax during the mounting procedure, causing small shifts in the relative positions of the two grips. We used the ball joint and the micromanipulator mount of the force beam to restore the initial muscle length and orientation. The position of the muscle was adjusted until both cut edges of both acetate strips were just touching and exactly aligned. The force beam manipulator was then locked in position and the retaining nut of the ball joint was tightened to prevent movement of the posterior grip. Finally, the acetate strips were trimmed away to prevent mechanical interference with imposed muscle length changes.

Temperature measurement and control

We measured thoracic temperature to the nearest 0.1°C using a 0.15 mm-diameter copper–constantan thermocouple inserted into the dl_1 muscles through a small hole in the cuticle. The entire experimental apparatus was enclosed within an insulated plywood box. Heated water circulating through

copper pipe within the box allowed us to maintain thorax temperature at 36±0.5°C. All twitch length–tension measurements were carried out at 36°C, the minimum thoracic temperature required for flight (Heinrich and Bartholomew, 1971; McCrea and Heath, 1971).

Muscle stimulation

We elicited twitches using bipolar, supramaximal stimuli, 0.2 ms in duration, delivered through a pair of stainless steel minuten pins. The minutens were inserted through the anterior notum and into the dl_1 muscles, one on ether side of the midline. In the intact thorax preparation, spurious stimulation of the antagonistic dorsoventral muscles required a doubling of the stimulus amplitude, and the resulting forces were clearly evident as both an upwards deflection of the wings combined with a reversal in the sign of the recorded twitch force. Stimuli were delivered continuously, at a frequency of 10 Hz. At this frequency there was no detectable fusion between successive twitches.

Measurement protocol and analysis: intact thorax and isolated muscles

We used both isolated muscle and intact thorax preparations to examine the effects of length on active twitch force. Twitch forces were digitized at a sample rate of 2 kHz. In all cases, we report the active twitch force, the peak force relative to the baseline for each twitch.

To examine the effects of muscle length on active twitch force, we changed muscle length in steps of 0.1 mm (isolated muscle) or 0.2 mm (intact thorax). We recorded either one or two complete ascending and descending length series from each preparation. In the isolated muscle preparations, we recorded active twitch forces over a range of lengths from 0.84 to 1.15 L_{max}. In the intact thorax preparation, the minimum length was L_r since the probes did not allow us to apply compressive forces to the muscle.

At the conclusion of each experiment, we used the calibrated micrometer on the translation stage to return the dl_1 muscles to their initial length. Two strips of stainless steel shim, one on each side, were glued across the gap separating the grips, securing the muscle at its initial length. We then removed the preparation from the experimental apparatus and dissected away the thorax surrounding the dl_1 muscles, leaving the muscles and their sites of attachment in place between the two grips. Using digital calipers, we measured the distance between the ventral and medial margins of the 1st and 2nd phragmata to the nearest 0.01 mm. The dl_1 muscles of one side were dissected free of the thorax and placed in *Manduca* saline (Tublitz and Truman, 1985). We recorded a video image of the medial aspect of the intact, contralateral dl_1 muscles. The remaining dl_1 muscles were then dissected free of the thorax and also placed in saline. Finally, the muscles were blotted dry and weighed together to the nearest 0.001 g. We calculated muscle volume from the measured muscle mass, assuming a muscle density of 1 g cm^{-3}. To calculate mean fiber length, we used six measurements of fiber length taken at evenly spaced intervals across the medial surface of the dl_1 muscles on the video image. We calculated the combined cross-sectional area of the two dl_1 muscles from the muscle volume divided by the mean fiber length.

To generate length–tension curves from the isolated muscle and intact thorax preparations, we first fit 2nd order polynomial curves (polyfit; Matlab) to the individual twitch length–tension data sets, then averaged the polynomial coefficients for all individuals within each of the two types of preparations. We determined the length at maximum force, $\mathbf{F}_{max}$, from the polynomial fit of the length–tension data for each individual.

Results

Body mass, muscle length and muscle mass

The 17 moths used in our measurements had a mean body mass of 1.83±0.26 g (S.D.). The anatomical rest length of the dl_1 muscles used in the tethered flight and *in situ* force–length measurements was 10.4±1.5 mm (±S.D.; N=12). The combined mass of the left and right dl_1 muscles from the moths used for isometric twitch force measurements either *in situ* or from mechanically isolated muscles was 0.164±0.02 g (±S.D.; N=11).

Muscle strain and activation phase in vivo

The moths used in our tethered flight measurements initiated pre-flight warm-up either spontaneously or in response to gentle prodding with a wooden applicator stick. Following an initial 5–10 min warm-up period, the moths switched to the large-amplitude wing stroke characteristic of normal flight. All data were collected during sustained flight bouts, at least 15–20 min following the initiation of flight behavior.

We selected flight sequences for detailed analysis if the dl_1 muscles fired continuously in every wing stroke, wing-beat frequency was 20 Hz or higher, and the video record showed that stroke amplitude was large and relatively constant. From these sequences, we analyzed one representative flight sequence for each of six moths (Table 1). The selected sequences were 59–106 wing-beats in duration with wing-beat frequencies of 21.1–25.6 Hz.

Length changes of the dl_1 muscles were approximately sinusoidal (Fig. 3). To compare the spectral composition of the muscle strain records across individuals, we normalized the Fourier-transformed data to the fundamental frequency. Distortion of the strain waveform, measured as the amplitude of the 2nd harmonic expressed as a percentage of the 1st harmonic, varied from 5.5 to 46%, with a mean of 25±17% (S.D.; N=6; Fig. 4; Table 1).

During flight, there was a net shortening of the dl_1 muscles so that, on average, L_{op} was 0.98±0.02L_r (S.D.; N=6). In each wing stroke, the total peak-to-peak amplitude of muscle strain was 0.09±0.02L_{op}. In five of the six moths, lengthening lasted slightly longer than shortening. On average, the duration of muscle shortening was 45±5% of the cycle period. The dl_1 muscles typically fired just before the onset of muscle shortening, with an average phase, relative to the muscle length change cycle, of 0.49±0.04.

Table 1. *Summary of the strain and timing of activation of the dl$_1$ muscles recorded during flight*

Moth	Wing-beat frequency (Hz)	Phase of activation	L_{op}/L_r	Strain amplitude ($\Delta L/L_o$)	Shortening duration (%)	f_2 (% of f_1)	N
1	25.6±0.8	0.45±0.02	0.99	0.055±0.003	46±2	5.5	59
2	22.3±0.8	0.49±0.02	0.95	0.125±0.005	60±4	29	106
3	23.5±0.4	0.48±0.01	0.99	0.065±0.001	44±1	46	93
4	23.2±0.8	0.56±0.03	0.96	0.131±0.005	54±1	12	92
5	22.4±0.6	0.50±0.03	0.97	0.040±0.003	47±3	13	88
6	21.1±0.5	0.45±0.01	1.00	0.080±0.004	41±2	42	105
Mean	23.0±1.5	0.49±0.04	0.98±0.02	0.090±0.031	45±5	25±17	

All values were calculated for each wing stroke cycle and averaged for the total number (N) of complete cycles within each flight bout. Phase of activation is the time from the start of muscle lengthening to the peak of the spike in the EMG record, divided by the cycle period. L_{op} is the operational muscle length, defined as the midpoint between the maximum and minimum length in each cycle. L_r is the rest length of the dl$_1$muscles. ΔL is the difference between the maximum and minimum length in each cycle. Shortening duration is the duration of muscle shortening expressed as a percentage of each cycle period. The amplitude of the 2nd harmonic of the Fourier-transformed strain record is expressed as a percentage (f_2) of the amplitude of the 1st harmonic. Values are given as means ± S.D.

Operating range of the dl$_1$ muscles on their twitch length–tension curve

The mean ratio of the anatomical rest length to the length at maximum isometric tension (L_r/L_{max}) measured in intact thorax preparations was 0.91±0.03 (S.D.; N=7). This ratio and the ratio L_{op}/L_r from our *in vivo* length experiments enabled us to calculate an estimate of the position of L_{op} on the isometric twitch length–tension curve: $L_{op}/L_{max}=(L_{op}/L_r)(L_r/L_{max})$. Based on this calculation, the mean L_{op} of the dl$_1$ muscles was $0.89\pm0.04L_{max}$ (Fig. 5). This L_{op}, together with the average peak-to-peak *in vivo* strain amplitude of $0.09\pm0.02L_{op}$, indicates that the dl$_1$ muscles operate entirely on the ascending limb of their twitch length–tension curve, over a range of $0.85–0.93L_{max}$ (Fig. 5). Because the configuration of the muscle grips used for twitch measurements in the intact thorax did not permit us to shorten the dl$_1$ muscles, this operational length range lies almost entirely below the length range of our isometric twitch measurements. Our results do, however, indicate that within the operating length range during flight, the maximum isometric twitch force in the intact thorax was only $0.72\mathbf{F}_{max}$. On the length–tension curve measured from mechanically isolated muscles, the length range of $0.85–0.93L_{max}$ corresponds to isometric twitch forces of $0.08–0.79\mathbf{F}_{max}$.

The length–tension curves measured by the two different methods were not identical. The intact thorax preparation produced a somewhat narrower length–tension curve, and the

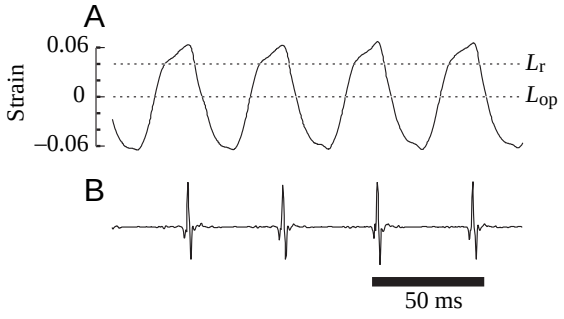

Fig. 3. (A) Strain and (B) electromyogram (EMG) signals recorded from the dl$_1$ muscle during tethered flight. In the sequence shown, the rest length in the quiescent moth (L_r; upper broken line) is 4% longer than the operational length (L_{op}; lower broken line). The dl$_1$ muscles fired a single spike near the onset of muscle shortening in each wing-stroke. The time scale (ordinate) is the same for both traces. The wing-stroke frequency in this sequence was 23 Hz (Table 1, moth 4).

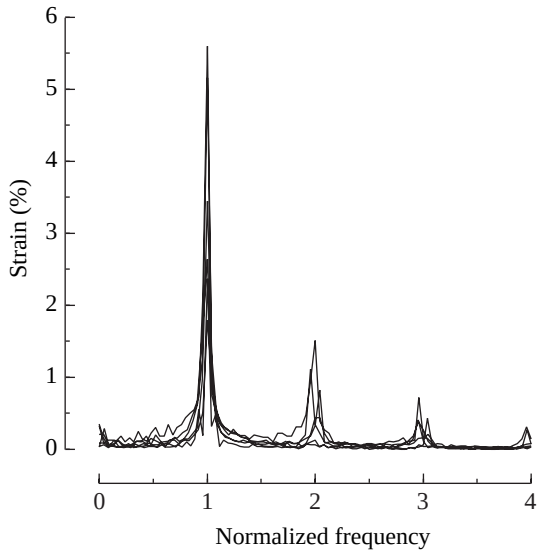

Fig. 4. Superimposed Fourier transforms of the strain records from six moths. For each flight sequence, the frequency values (abscissa) have been normalized by dividing the frequency of the first (dominant) Fourier coefficient by the wing-beat frequency of that trial. The mean distortion of the strain trajectories from sinusoidal was 25±17% as measured by the ratio of the dominant coefficient to that of the first harmonic.

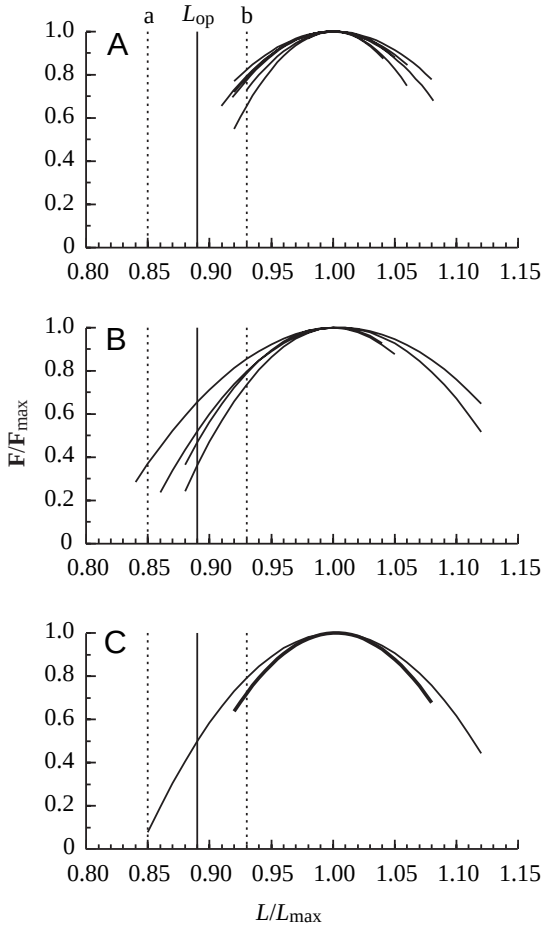

Fig. 5. Isometric twitch length–tension curves derived from active twitch forces measured from the dl_1 muscles. The dl_1 muscles operate exclusively on the ascending limb of their length–tension curve. (A) Isometric twitch length–tension curve based on *in situ* measurements from the intact thoraces of seven moths. (B) Isometric twitch length–tension curves measured from mechanically isolated dl_1 muscles from four moths. (C) Length–tension curves representing pooled data from intact thorax preparations (heavy line) and from isolated muscle preparations (light line). All curves in A and B are 2nd order polynomials fit to individual data sets. Each curve in C was obtained by averaging the polynomial coefficients from the individual curves within each of the two data sets shown in A and B. The solid vertical line in each plot indicates the mean value of operational length (L_{op}), measured relative to the anatomical rest length of the dl_1 muscles in six tethered flight preparations. The broken vertical lines (a, mean minimum muscle length; b, mean maximum muscle length) indicate the average bounds of muscle length changes during tethered flight. Muscle length for active twitch force measurements in the intact thorax preparations (A) was also referenced to the anatomical rest length. This common length reference allowed us to map the *in vivo* muscle length changes measured in tethered flight onto the twitch length–tension curve measured in intact thorax preparations (A). The vertical lines indicating L_{op} and the mean range of length changes derived from measurements in tethered flight and from the intact thorax preparation are replicated in B and C. Although the intact thorax and isolated muscle preparations produced different curves, both indicate that active twitch force is substantially lower than maximal over the range of *in vivo* muscle lengths.

mean value of peak stress at L_{max} was 32±8 kPa (S.D.; N=7), substantially lower than the corresponding value of 82±10 kPa (S.D.; N=4) measured from isolated muscles. These differences, however, do not qualitatively alter our results; in both cases, the L_{op} range falls entirely on the ascending limb of the length–tension curve, at muscle lengths where twitch forces were substantially lower than $\mathbf{F}_{max}$.

Discussion

The synchronous dl_1 muscles of *Manduca* undergo large amplitude strains and operate entirely on the ascending region of their twitch length–tension relationship. It is important to note that relatively few studies have combined measurements of both the L_{op} range and the length–tension relationship for the same muscle subject to physiological stimulation.

To interpret the functional consequences of operation on the ascending limb of the length–tension curve, we draw on comparisons with other muscle systems. Both cardiac muscle and the dl_1 muscles undergo cyclic strains at large amplitudes. The strain amplitude of the dl_1 muscles is considerably greater than the largest amplitudes reported to date for other insects: ~3% in the asynchronous wing elevator muscles of bumblebees (Josephson and Ellington, 1997). In these asynchronous muscles, molecular mechanisms associated with stretch activation may restrict the acceptable strains to rather low amplitudes (Dudley, 2002). When we compare the twitch length–tension curves of the dl_1 muscles and mammalian cardiac muscle (Fig. 6), we see a striking similarity in shape. Both curves have steep rising regions and narrow peaks. Moreover, both curves are considerably steeper and narrower than active twitch length–tension curves for vertebrate skeletal muscle. The insect synchronous muscle and the mammalian cardiac muscle also share the functional characteristic of operating entirely at lengths that fall on the ascending parts of their length–tension curves.

As with mammalian cardiac muscle, the combination of a steep twitch length–tension curve and a large operating range on the ascending region may have important regulatory consequences. Operation on the ascending limb of a steep length–tension curve gives mammalian cardiac muscle the capacity to generate the larger forces required by increases in ventricular filling. In an analogous manner, operation on the ascending limb of its steep length–tension curve may confer the ability of the dl_1 muscles to accommodate transient increases in wing stroke amplitude without the need for changes in neural control. Turning maneuvers by *Manduca* involve asymmetrical changes in both wing-stroke amplitude and the extent of pronation and remotion. These changes appear to be controlled by shifts in the phase and frequency of activation in the relatively small direct flight muscles, especially the basalar and axillary muscles (Kammer, 1971; Wendler et al., 1993; Rheuben and Kammer, 1987). Turning

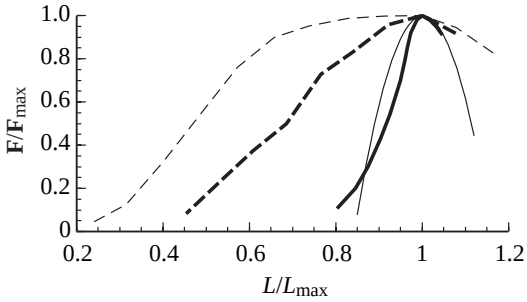

Fig. 6. Active twitch length–tension curve for the dl_1 muscles of *Manduca* (light solid line), mammalian cardiac muscle (heavy solid line; redrawn from Allen and Kentish, 1985), cat soleus muscle (light broken line; redrawn from Rack and Westbury, 1969) and the length–tension curve for tetanized cat soleus muscle (heavy broken line; redrawn from Rack and Westbury, 1969). Compared with mammalian skeletal muscle, the dl_1 muscles and mammalian cardiac muscle both have length–tension relationships with steep ascending regions and narrow peaks, even compared with mammalian skeletal muscle at low levels of activation. The curve for *Manduca* dl_1 muscles is the same as that shown for mechanically isolated muscles in Fig. 5C.

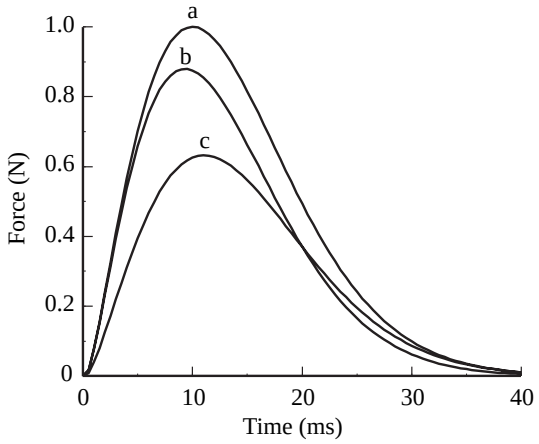

Fig. 7. The time course of a twitch force depends upon where along the length–tension curve the muscle operates. The twitch force ($\mathbf{F}_t$) was modeled with the function $\mathbf{F}_t=\exp[-1000(t-0.01)^2/t^{0.5}]$, where t is time in seconds. Force is plotted against time with (a) no length dependence of the force, (b) a length dependence of force that increases linearly in time with a strain ε of 0.5 [$\mathbf{F}_t(1-\varepsilon\ t/0.04)$; e.g. contraction on the ascending portion of the length–tension relationship] and (c) a length dependence that decreases linearly in time with the same strain as in b [$\mathbf{F}_t(1+\varepsilon\ t/0.04-\varepsilon)$; e.g. contraction on the descending portion of the length–tension relationship]. Operating along the ascending portion leads to an earlier peak and a more rapid decline in force.

maneuvers do not appear to involve substantial changes in the firing patterns of the indirect dl_1 muscles (Kammer, 1971). The dl_1 muscles, however, will almost certainly experience transient changes in strain amplitude as the altered motions of the wings are transmitted through the mechanical linkages of the thorax. The normally large amplitude strains in the dl_1 muscles, combined with a steep twitch length–tension curve, should confer a strong length dependence on force generation throughout the wing stroke. Moreover, because these length changes occur entirely on the ascending limb of the twitch length–tension curve, the capacity of the dl_1 muscles to generate force will rise sharply as the muscle is stretched. This characteristic of the dl_1 muscles could therefore provide an intrinsic mechanism to restore the amplitude of muscle length changes to their steady-state value following a transient increase in strain, even without an adjustment in the pattern of neural activation. The lowered capacity of the muscles to generate force that results from operation on the ascending limb of the twitch length–tension relationship (*vs* shortening across the plateau) suggests that such an intrinsic regulatory mechanism may involve a compromise between control and power generation. Intrinsic regulation of muscle contraction is generally thought to be a property restricted to asynchronous flight muscle, in which stretch activation decouples the amplitude and frequency of muscle contractions from direct neural control. Our results suggest that synchronous flight muscles could also have some degree of intrinsic regulation that depends on their cardiac-like mechanical behavior, even though their contraction frequency is tightly coupled to the frequency of neuronal firing.

The range of lengths over which a muscle contracts has a profound influence on the temporal patterns of its mechanical activity (Edman and Nilsson, 1971). Because calcium release occurs more quickly than uptake by the sarcoplasmic reticulum, twitch force rises much more rapidly than it declines.

For contraction at a constant velocity, this temporal asymmetry will result in greater shortening during the relatively longer falling phase than during the shorter rising phase of a twitch. Therefore, the effect of length dependence on force will be greater during the falling phase. For example, for muscle shortening that occurs entirely down the ascending limb of the length–tension curve, the decrement in force due to length dependence will be smaller through the short rising phase of a twitch than throughout the longer declining phase.

A muscle that twitches as it shortens along the ascending portion of the length–tension curve will reach a larger force more rapidly than a muscle contracting along the descending part of the curve. The subsequent decline in twitch force will also occur more rapidly. We illustrate this point using a model of a twitch of a muscle that is allowed to shorten, combined with a simple linear length dependence of the twitch force (Fig. 7).

Shortening deactivation may also be important in avoiding fusion in rapidly contracting cardiac muscles (Allen and Kentish, 1985). Isometric twitch forces produced by the dl_1 muscles of *Manduca* show a small degree of fusion when stimulated at wing-stroke frequency (25 Hz), even in their normal operating temperature range of 36–40°C. Reduced twitch duration due to shortening deactivation may augment the net power output by reducing active force generation as the muscle is stretched (negative work).

We do not know the extent to which cardiac-like mechanical behavior may occur in other skeletal muscle systems. Frog jumping muscles appear to operate on the plateau of their length–tension relationship (Lutz and Rome, 1994). These muscles, however, power explosive, ballistic motions. Among muscles that power sustained, cyclic activity, cardiac-like mechanics could provide non-neuronal mechanisms for regulating the excursion of oscillating legs, wings or other appendages. Although there are no other additional data for synchronous insect flight muscles, both a crab flagellar muscle (Josephson and Stokes, 1987) and scallop abductor muscle (Olson and Marsh, 1993) operate at lengths shorter than those corresponding to maximum twitch or tetanic force generation. Intriguingly, the steep tetanic length–tension relationship of crab flagellar muscle is similar to those of mammalian cardiac muscle and the dl_1 muscles of *Manduca* (Josephson and Stokes, 1987). Contrary data for fish, however, suggest that the muscles that power sustained swimming operate on the plateau region of their tetanic length–tension relationship (Rome and Sosnicki, 1991). Clearly, given the surprising paucity of similar data sets, generalities may be premature.

We often assume that the shape and slope of the classic length–tension relationship published by Gordon et al. (1966) is a general characteristic of striated skeletal muscle. Indeed, the conservative range of sarcomere lengths found among vertebrate striated muscles lends credence to this assumption. However, a host of data suggests that factors other than filament geometry alone (and therefore sarcomere lengths) can alter the slope of the length–tension relationship: swapping troponins between cardiac and skeletal muscles, changing the concentration of extracellular calcium around cardiac cells, and even altering the level of activation for skeletal muscle, can all change the slope of the length–tension relationship (Gordon et al., 2000). These findings, taken together with our results, suggest that the mechanical behavior of locomotor muscles may vary considerably more than previously thought. Although largely unexplored, such potential variation suggests a possible range of mechanisms for tuning muscle contractile performance to the specific functional needs of animal locomotion.

We wish to thank Stacey Combes and Sanjay Sane for critical comments on the manuscript. This work was supported by NSF Grant 9511681 to T.L.D., a Packard Interscience Grant to T.L.D. and an ONR MURI Grant.

References

Allen, D. G. and Kentish, J. C. J. (1985). The cellular basis of the length-tension relation in cardiac muscle. *J. Mol. Cell. Cardiol.* **17**, 821-840.

Biewener, A. A., Corning, W. R. and Tobalske, B. W. (1998). *In vivo* pectoralis muscle force-length behavior during level flight in pigeons (*Columba livia*). *J. Exp. Biol*. **201**, 3293-3307.

Burkholder, T. J. and Lieber, R. L. (2001). Sarcomere length operating range of vertebrate muscles during movement. *J. Exp. Biol*. **204**, 1529-1536.

Dial, K. P. and Biewener, A. A. (1993). Pectoralis muscle force and power output during different modes of flight in pigeons (*Columba livia*). *J. Exp. Biol*. **176**, 31-54.

Chan, W. P. and Dickinson, M. H. (1996). *In vivo* length oscillations of indirect flight muscles in the fruit fly *Drosophila virilis*. *J. Exp. Biol*. **199**, 2767-2774.

Dudley, R. (2002). *The Biomechanics of Insect Flight*. Princeton: Princeton University Press.

Eaton, J. L. (1988). *Lepidopteran Anatomy*. New York: Wiley Interscience.

Edman, K. A. and Nilsson, E. (1971). Time course of the active state in relation to muscle length and movement: a comparative study on skeletal muscle and myocardium. *Cardiovasc. Res.* **1 (Suppl. 1)**, 3-10.

Gilmour, K. M. and Ellington, C. P. (1993). *In vivo* muscle length changes in bumblebees and the *in vitro* effects on work and power. *J. Exp. Biol*. **183**, 101-113.

Gordon, A. M., Huxley, A. F. and Julian, F. J. (1966). The variation in isometric tension with sarcomere length in vertebrate muscle fibers. *J. Physiol.* **184**, 170-192.

Gordon, A. M., Homsher, E. M. and Regnier, M. (2000). Regulation of contraction in striated muscle. *Physiol. Rev*. **80**, 853-924.

Heinrich, B. and Bartholomew, G. A. (1971). An analysis of pre-flight warm-up in the sphinx moth *Manduca sexta*. *J. Exp. Biol.* **55**, 223-239.

Josephson, R. K. and Stokes, D. R. (1987). The contractile properties of a crab respiratory muscle. *J. Exp. Biol.* **131**, 265-287.

Josephson, R. K. and Ellington, C. P. (1997). Power output from a flight muscle of the bumblebee *Bombus terrestris* I. Some features of the dorso-ventral flight muscle. *J. Exp. Biol*. **200**, 1215-1226.

Josephson, R. K., Malamud, J. G. and Stokes, D. R. (2000). Asynchronous muscle: a primer. *J. Exp. Biol*. **203**, 2713-2722.

Kammer, A. E. (1971). The motor output during turning flight in a hawkmoth, *Manduca sexta*. *J. Insect Physiol.* **17**, 1073-1086.

Kammer, A. E. (1985). Flying. In *Comprehensive Insect Physiology, Biochemistry and Pharmacology*, vol. 5 (ed. G. A. Kerkut and L. I. Gilbert), pp. 491-552. New York: Pergamon Press.

Layland, J., Young, I. A. and Altringham, J. D. (1995). The length dependence of work production in rat papillary muscles in vitro. *J. Exp. Biol.* **198**, 2491-2499.

Lutz, G. J. and Rome, L. C. (1994). Built for jumping: the design of the frog muscular system. *Science* **263**, 370-372.

McCrea, M. J. and Heath, J. E. (1971). Dependence of flight on temperature regulation in the moth, *Manduca sexta*. *J. Exp. Biol.* **54**, 415-435.

Nüesch, H. (1953). The morphology of the thorax of *Telea Polyphemus* (Lepidoptera). I. Skeleton and muscles. *J. Morph. Philadelphia* **93**, 589-608.

Olson, J. M. and Marsh, R. L. (1993). Contractile properties of the striated adductor muscle in the bay scallop *Argopectten irradians* at several temperatures. *J. Exp. Biol.* **176**, 175-193.

Rack, P. M. H. and Westbury, D. R. (1969). The effects of length and stimulus rate on tension in the isometric cat soleus muscle. *J. Physiol.* **204**, 443-460.

Rheuben, M. B. and Kammer, A. E. (1987). Structure and innervation of the third axillary muscle of *Manduca* relative to its role in turning flight. *J. Exp. Biol*. **131**, 373-402.

Rome, L. C. and Sosnicki, A. A. (1991). Myofilament overlap in swimming carp. II. Sarcomere length changes during swimming. *Am. J. Physiol.* **260**, C289-C296.

Wendler, G. Muller, M. and Dombrowski, U. (1993). The activity of pleurodorsal muscles during flight and at rest in the moth *Manduca sexta* (L.). *J. Comp. Physiol. A* **173**, 65-75.

Williamson, M. R., Dial, K. P. and Biewener A. A. (2001). Pectoralis muscle performance during ascending and slow level flight in mallards (*Anas platyrhynchos*). *J. Exp. Biol.* **204**, 495-507.

Tublitz, N. J. and Truman, J. W. (1985). Identification of neurons containing cardioacceleratory peptides (CAPS) in the ventral nerve cord of the tobacco hawkmoth, *Manduca-sexta*. *J. Exp. Biol*. **116**, 395-410.